JOURNAL OF AGRICULTURAL AND FOOD CHEMISTRY

pubs.acs.org/JAFC Article

Engineering Bacillus subtilis Isoleucine Dioxygenase for Efficient Synthesis of (2*S*,3*R*,4*S*)-4-Hydroxyisoleucine

Ping Du, Shuai Yan, Xiao-Long Qian, Jiang Pan, Zhi-Jun Zhang,* Hui-Lei Yu,* and Jian-He Xu*

Cite This: https://dx.doi.org/10.1021/acs.jafc.0c06544 Read Online

ACCESS | Metrics & More | Article Recommendations | Supporting Information

ABSTRACT: Isoleucine dioxygenase (IDO)-catalyzed hydroxylation of isoleucine is a promising method for the synthesis of the diabetic drug (2*S*,3*R*,4*S*)-4-hydroxyisoleucine [(2*S*,3*R*,4*S*)-4-HIL]. However, the low activity of IDO significantly limits its practical application. In this work, a high-throughput screening method was developed and directed evolution was performed on the IDO from *Bacillus subtilis*, resulting in a double mutant with improvements in specific activity, protein expression level, and fermentation titer of 3.2-, 2.8-, and 9.4-fold, respectively. L-Isoleucine (228 mM) was completely converted to (2*S*,3*R*,4*S*)-4-HIL by the best variant with a space-time yield of up to 80.8 g L^{-1} d^{-1}, which is the highest record reported so far. With a further increase of the substrate loading to 1 M, a high conversion of 91% could also be achieved. At last, enzymatic synthesis of (2*S*,3*R*,4*S*)-4-HIL was successfully carried out on a 3 L scale, indicating tremendous potential of the IDO variant I162T/T182N for green and efficient production of (2*S*,3*R*,4*S*)-4-HIL.

KEYWORDS: *biocatalysis, isoleucine dioxygenase, directed evolution, (2S,3R,4S)-4-hydroxyisoleucine, space-time yield*

INTRODUCTION

4-Hydroxyisoleucine (4-HIL), a natural nonproteinogenic amino acid, was initially isolated from fenugreek seeds.[1] Further studies have shown that 4-HIL is capable of promoting insulin secretion with a strict dependence on the glucose concentration, that is, when the glucose concentration is above 8 mM, 4-HIL can trigger insulin secretion.[2,3] Because there are three asymmetric carbons in 4-HIL, eight diastereomers and four pairs of enantiomers are possible. However, (2*S*,3*R*,4*S*)-4-HIL was demonstrated to be the most effective among the eight diastereomers.[4] Furthermore, besides promoting insulin secretion, (2*S*,3*R*,4*S*)-4-HIL can also improve insulin resistance and reduce blood fat.[5−9] Therefore, (2*S*,3*R*,4*S*)-4-HIL is considered to be one of the most promising oral drugs for the treatment of diabetes,[10] especially for its unique feature of strict glucose-induced release of insulin, which would significantly reduce the undesirable side effects commonly observed for the other pharmaceutical drugs in the treatment of diabetes.

Because of the remarkable importance of (2*S*,3*R*,4*S*)-4-HIL in the treatment of diabetes, several methods for the preparation of (2*S*,3*R*,4*S*)-4-HIL have been developed. Originally, (2*S*,3*R*,4*S*)-4-HIL was isolated from fenugreek seeds. However, the extraction method requires complicated purification steps with a very low isolated yield,[1,6] for example, approximately 100 g of (2*S*,3*R*,4*S*)-4-HIL could only be obtained from 110 kg of fenugreek seeds. Moreover, a cultivated field of 300 m^2 is required to produce 110 kg of fenugreek seeds for 9 months, indicating that the extraction method is not suitable for the large-scale preparation of (2*S*,3*R*,4*S*)-4-HIL. In addition to the extraction method, chemical and enzymatic methods have also been developed; however, the low yields, complicated synthesis steps, unsatisfactory stereoselectivity, and serious environmental pollution substantially limit their practical application.[11−15] In contrast to the above-mentioned methods, the isoleucine dioxygenase (IDO)-catalyzed hydroxylation of L-isoleucine (L-Ile) represents a green and straightforward strategy (Scheme 1). It is noteworthy that the reaction proceeds with excellent regioselectivity and stereoselectivity, and only one diastereomer, (2*S*,3*R*,4*S*)-4-HIL, was produced.[16] Indeed, the IDO-mediated hydroxylation of L-Ile has received increasing attention in recent years, and IDOs from different microorganisms have been applied in the synthesis of (2*S*,3*R*,4*S*)-4-HIL.[17−20] However, the poor catalytic activity of IDOs makes their practical application still an unmet challenge.

Scheme 1. IDO-Catalyzed Synthesis of (2*S*,3*R*,4*S*)-4-HIL

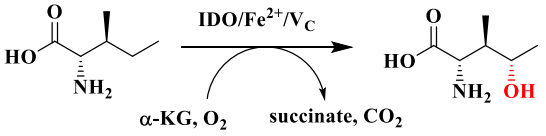

Recently, protein engineering has emerged as a powerful tool in tuning enzyme properties,[21] including catalytic activity,[22] substrate spectrum,[23] selectivity,[24,25] thermostability,[26] and new reaction types.[27] The same strategy has also been applied in the engineering of IDOs aiming to improve

Received: October 14, 2020
Revised: November 16, 2020
Accepted: November 18, 2020

https://dx.doi.org/10.1021/acs.jafc.0c06544
J. Agric. Food Chem. XXXX, XXX, XXX−XXX

Scheme 2. High-Throughput Screening Method Coupling IDO with 4-HIL Dehydrogenase

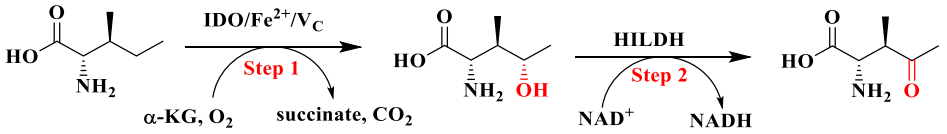

their catalytic activities. For example, an enhancement of 1.5-fold in the catalytic efficiency of IDO from *Bacillus thuringiensis* TCCC 11826 was achieved by directed evolution, in which the improved variants were identified through restoration of cell growth of the succinate-auxotrophic *E. coli* by coupling the hydroxylation of L-Ile and the oxidation of α-ketoglutarate to succinate.[28] Although this strategy is easy for screening beneficial mutants by simply observing the growth of cells, it requires complicated genetic manipulation of the host cells and the false positive is relatively high. In the case of IDO from *B. weihenstephanensis* KBAB4, paper chromatography was used for the detection of (2*S*,3*R*,4*S*)-4-HIL produced from an IDO random mutagenesis library, resulting in the identification of a double mutant N126H/T130K with a 2.4-fold improvement in catalytic efficiency.[29] However, this method is not suitable for high-throughput screening because it requires cumbersome operation and is time-consuming. The specific activity of the IDO from *B. cereus* 13658 was increased by 3.5-fold by introducing a disulfide bond into the protein structure.[30] Although great efforts have been made to increase the catalytic efficiency of IDO by protein engineering, the improvement is somewhat limited. There are two main reasons accounting for this phenomenon: first, not only the crystal structure of any currently known IDOs has not been resolved so far but also there is no homologous protein structure available in the protein data bank. Therefore, only the more random error-prone polymerase chain reaction (ep-PCR) other than semirational or rational design could be used for the engineering of IDO. Second, a relatively small-capacity mutant library with limited diversity could be screened because of the lack of a high-throughput screening method, which would severely reduce the positive hits in the screening of the mutant library.

In this work, a high-throughput screening method via a (2*S*,3*R*,4*S*)-4-HIL dehydrogenase (HILDH)-coupled UV assay for IDO activity was developed and was successfully employed for the identification of improved variants from a random mutant library of IDO from *B. subtilis* (Scheme 2). Finally, a double mutant I162T/T182N, which simultaneously increases the specific activity and protein expression level of IDO, was obtained by a combination of beneficial mutations. Enzymatic synthesis of (2*S*,3*R*,4*S*)-4-HIL by the best mutant gave the highest space-time yield(STY) reported so far. Furthermore, the high-throughput screening method and the engineering strategy might be applicable to the directed evolution of other amino acid dioxygenases, a group of important enzymes without crystal structures available.

MATERIALS AND METHODS

Strains, Plasmids, and Materials. The IDO (UniProt ID: A0A246PI45) from *B. subtilis* was used as a template. The plasmid pET-28a (+) and *E. coli* BL21 (DE3) were used as the expression vector and host cell for IDO and its mutants, respectively. PrimeSTAR HS DNA polymerase, restriction enzymes, and T_4 DNA ligase were purchased from TaKaRa (Dalian, China). L-Ile was kindly provided by Wuxi Jinghai Amino Acid Co., Ltd. (Wuxi, China). 4-HIL and (2*S*,3*R*,4*S*)-4-HIL were purchased from Macleans (Shanghai, China). The macroporous strong acidic cation-exchange resin (D001) was kindly donated by Shanghai Huazhen Technology Co., Ltd.

Construction of a Random Mutagenesis Library. The mutant library of IDO was constructed using the plasmid pET28a-IDO as the template for PCR amplification (Tables S1 and S2) with IDO-F and IDO-R as the primers (Table S3). After being purified and digested with *EcoR* I and *Hind* III, the PCR products were ligated into the *EcoR* I and *Hind* III restriction sites of pET-28a (+), and the resultant recombinant plasmid was then transformed into the competent cells of *E. coli* BL21 (DE3) to give the random mutant library of IDO.

Establishment of a High-Throughput Screening Method for IDO. In 2011, an NAD^+-dependent (2*S*,3*R*,4*S*)-4-HIL dehydrogenase (HILDH) was discovered from the *B. thuringiensis* ATCC 35646 strain,[31] which can catalyze the oxidative dehydrogenation of 4-HIL to 4-oxo-isoleucine and meanwhile reduce NAD^+ to NADH. The amount of NADH produced equals to that of 4-HIL consumed by HILDH. Therefore, a high-throughput screening method was developed by coupling IDO with HILDH, in which isoleucine was first hydroxylated by IDO to produce (2*S*,3*R*,4*S*)-4-HIL, and the latter was then dehydrogenated by HILDH to 4-oxo-isoleucine with the concurrent reduction of NAD^+ to NADH (Scheme 2). As a result, the activity of IDO could be quantified by measuring the absorbance of NADH at 340 nm using a microtiter plate reader.

In order to verify the feasibility of the high-throughput screening method for library screening, different concentrations (0.1−0.9 mM) of (2*S*,3*R*,4*S*)-4-HIL were added to the reaction mixture composed of 10 mM L-Ile, 10 mM α-KG, 0.05 mM V_C, 0.05 mM Fe^{2+}, 4 mM NAD^+, 3 U HILDH, and 100 mM and pH 7.0 KPB, and the absorbance at 340 nm was measured within 1 min. In addition, different amounts of the IDO cell-free extract were used for the first hydroxylation step (a 500 μL reaction system: 10 mM L-Ile, 10 mM α-KG, 0.05 mM Fe^{2+}, 0.05 mM V_C, and 100 mM and pH 7.0 KPB), and after 1 h of reaction, 20 μL of the reaction solution was taken for the second step of dehydrogenation (a 200 μL reaction system: 4 mM NAD^+, 3 U HILDH, and 100 mM and pH 7.0 KPB), and the absorbance at 340 nm was measured within 3 min.

Screening of the Mutant Library. Colonies from the mutant library were picked to inoculate 600 μL of the Luria-Bertani (LB) medium (50 μg/mL kanamycin) in 96 deep-well plates. After overnight culture at 37 °C, 60 μL of the seed culture was used to inoculate 600 μL of the fresh LB medium in 96 deep-well plates. The plates were incubated at 37 °C for 3 h, and protein expression was induced at 16 °C for 24 h with the addition of 0.2 mM Isopropyl-β-D-thiogalactopyranoside (IPTG). Cells were harvested by centrifugation and lysed by adding 200 μL of the lysis buffer [0.75 mg/mL lysozyme (BIOFROXX, 20000 U/mg) and 0.01 mg/mL DNase I (MACKLIN, 2000 U/mg)], followed by freeze-thawing. The plates were centrifuged at 3400*g* for 20 min to remove the cell debris, and the supernatant was used as a cell-free extract. To screen the positive mutants with improved IDO activity, the previously established high-throughput screening method was applied. First, 20 μL of the cell-free extract was added to 480 μL of the reaction solution (100 mM and pH 7.0 KPB, 10 mM L-Ile, 10 mM α-KG, 0.05 mM V_C, and 0.05 mM Fe^{2+}) in 96 deep-well plates, and the resultant mixture was shaken at 30 °C for 1 h. Second, the reaction mixture was centrifuged, and 20 μL of the supernatant was added to 180 μL of the dehydrogenation reaction solution (4 mM NAD^+, 3 U HILDH, and 100 mM and pH 7.0 KPB) in 96-well microtiter plates, and the absorbance within 3 min was detected at 340 nm. The mutants with higher absorbance

https://dx.doi.org/10.1021/acs.jafc.0c06544
J. Agric. Food Chem. XXXX, XXX, XXX−XXX

than the wild-type enzyme were selected for rescreening with respect to expression level and specific activity.

Expression and Purification of Wild-Type IDO and Its Mutants. The recombinant *E. coli* BL21 (DE3) cells were grown at 37 °C and 180 rpm until the OD_{600} reached 0.6−0.8. IPTG was added to a final concentration of 0.2 mM, and the cultivation was continued at 16 °C and 180 rpm for another 24 h. The cells were harvested, washed twice with saline, and resuspended in ice-chilled buffer A (25 mM KPB, 300 mM NaCl, 10 mM imidazole, pH 8.0) to a final concentration of 0.05 g/mL, and then, the cells were disrupted by sonication. The cell lysate was centrifuged at 4 °C and 8000*g* for 30 min, and the supernatant was collected as the cell-free extract of IDO. The supernatant was loaded onto a His-Trap Ni-nitrilotriacetic acid FF column (5 mL; GE Healthcare Co.) pre-equilibrated with buffer A. The target protein was eluted using an increasing gradient of imidazole from 10 to 200 mM at a flow rate of 5 mL/min and detected by sodium dodecyl sulfate (SDS)-polyacrylamide gel electrophoresis (PAGE). The fraction containing the purified protein was collected and concentrated by ultrafiltration. The freshly purified enzyme was then used for further experiments.

Site-Directed Mutagenesis. Site-directed mutagenesis was conducted using the recombinant plasmid of pET 28a-IDO as the template with primers listed in Table S4. PCR amplification conditions are shown in Tables S1 and S2.

Enzyme Assay. The assay mixture containing 10 mM L-Ile, 10 mM α-KG, 0.5 mM Fe^{2+}, and 0.5 mM Vc in 100 mM KPB buffer (pH 7.0) was incubated with wild-type IDO or its variants at 30 °C for 30 min. The reaction solution was added with an equal volume of acetonitrile to terminate the enzyme reaction. The resultant solution was subsequently subjected to derivatization pretreatment, and the concentration of (2*S*,3*R*,4*S*)-4-HIL was determined by high-performance liquid chromatography (HPLC). One unit of enzyme activity was defined as the amount of enzyme required to produce 1 μmol of (2*S*,3*R*,4*S*)-4-HIL under the assay conditions.

2,3,4,6-Acetyl-β-*D*-glucopyranosyl isothiocyanate (GITC) precolumn derivatization method: the reaction solution was added with an equal volume of acetonitrile to terminate the reaction, and the denatured protein was removed by centrifugation. 100 μL of the supernatant was transferred into a 2 mL Eppendorf tube, to which 150 μL of acetonitrile−water−triethylamine solution (5 mL−5 mL−40 mg) and 250 μL of GITC solution (5 mM, dissolved in acetonitrile) were added sequentially, and incubated at 30 °C for 30 min.

Characterization of IDO. The optimum temperature for enzyme activity was determined by performing assays at 20−50 °C and pH 7.0, and the optimum pH was measured by conducting assays at pH 5.0−10.0 at the optimum temperature. The buffers (100 mM) used were as follows: citric acid-sodium citrate (pH 5.0−6.0), potassium phosphate (pH 6.0−9.0), and Gly-NaOH (pH 9.0−10.5). The highest activity was normalized as 100%. To investigate the effect of metal ions on the activity of IDO, reactions were carried out in 100 mM KPB buffer (pH 7.0) containing 10 mM L-Ile, 10 mM α-KG, 0.5 mM V_C, 0.5 mM Fe^{2+}, purified enzyme, and 1 mM of the respective metal ion [Ca^{2+}, Mg^{2+}, Mn^{2+}, Zn^{2+}, Cu^{2+}, Ni^{2+}, Co^{2+}, Li^{+}, or ethylenediaminetetraacetic acid (EDTA)] at 30 °C for 5 min.

To investigate the thermostability of IDO, enzyme solutions (1.0 mg/mL) were incubated at different temperatures (30, 40, and 50 °C) in KPB for different periods, followed by the measurement of the residual activity. The activity of the enzyme before incubation was normalized as 100%.

Optimization of Reaction Conditions for IDO-Mediated Isoleucine Hydroxylation. The reaction conditions for the enzymatic preparation of (2*S*,3*R*,4*S*)-4-HIL were further optimized to improve the efficiency. For optimum pH, the reaction mixture (50 mL) containing 228 mM (30 g/L) L-Ile, 342 mM α-KG (1.5 equiv to isoleucine), 10.0 mM Fe^{2+}, and 10.0 mM V_C was adjusted to pH values of 6.5, 7.0, and 7.5, respectively, prior to the addition of 10 g/L IDO I162T/T182N wet cells. For optimum temperature, the reactions were carried out at 20, 30, and 40 °C, respectively, with a shaker speed of 200 rpm for 48 h, and the amount of the product (2*S*,3*R*,4*S*)-4-HIL produced in the reaction solution was analyzed by HPLC. The effect of α-KG on the conversion was also investigated at pH 7.0 and 30 °C with different amounts (0.5, 1.0, and 1.5 equiv to isoleucine) of α-KG supplemented to the reaction mixture. At last, the effect of cell loading on the conversion was studied under the conditions of optimal pH, temperature, and α-KG supplementation.

To evaluate the catalytic potential of the variant IDO I162T/T182N, reaction was carried out on a 50 mL scale with wild-type IDO as a control. The pH of the reaction mixture composed of 228 mM L-Ile, 342 mM α-KG, 10.0 mM Fe^{2+}, and 10.0 mM V_C was adjusted to 7.0 with 10 N NaOH prior to the addition of 10 g/L of both wild-type IDO and I162T/T182N in the form of wet cells, and incubation was carried out at 30 °C and 200 rpm. The amount of (2*S*,3*R*,4*S*)-4-HIL produced was analyzed by HPLC.

Analytical Methods. L-Ile and (2*S*,3*R*,4*S*)-4-HIL were analyzed by HPLC with a UV detector at 254 nm and a reverse-phase Nucleosil C18 column (Hypersil ODS2, 4.6 × 250 mm, 5 μm), and the column was eluted at a flow rate of 0.8 mL min^{-1} with a solvent system of methanol/water (55/45, v/v) at 30 °C.

(2*S*,3*R*,4*S*)-4-HIL isomers were analyzed by HPLC with a UV detector at 250 nm and a reverse-phase Nucleosil C18 column (Hypersil ODS2, 4.6 × 250 mm, 5 μm) at 45 °C with a 10 mM, pH 2.8 KH_2PO_4 (eluent A) and acetonitrile (eluent B) solvent system at a flow rate of 0.3 mL min^{-1} in 0−60 min for 20−25% (v/v) B and 25% (v/v) B in 60.1−70 min.

RESULTS AND DISCUSSION

Development of a High-Throughput Screening Method for IDO. A high-throughput screening method plays a vital role in the identification of improved variants from a large mutant library,[32] especially for the directed evolution of enzymes without protein structure information available. In order to develop a high-throughput screening method for IDO, a dehydrogenase-coupled assay was adopted (Scheme 2). The activities of the IDO variants were inferred from the coupled rate of the NAD^+ turnover by (2*S*,3*R*,4*S*)-4-HIL dehydrogenase, which was dependent on the amount of (2*S*,3*R*,4*S*)-4-HIL formed by IDO. Formation of NADH by concurrent reduction of NAD^+ was detected by the change in absorbance at 340 nm using a spectrophotometer.[33]

To verify the linearity of (2*S*,3*R*,4*S*)-4-HIL concentration with the optical absorbance at 340 nm, different concentrations of the (2*S*,3*R*,4*S*)-4-HIL commercial sample were added to the standard reaction mixture and measured by the colorimetric assay using a microtiter plate reader. A linear relationship between the absorbance at 340 nm and (2*S*,3*R*,4*S*)-4-HIL concentration was observed from 0.1 to 0.9 mM (Figure 1A), which allows for the continuous quantification of the IDO activity based on the calibration curve. To further validate the feasibility of this method for screening the mutant library containing IDO variants with diverse activities, different amounts of IDO were added to the assay mixture and the absorbance at 340 nm was measured. Meanwhile, to prevent possible background interference, a lower concentration of Vc and Fe^{2+} (0.05 mM) was adopted. As can be seen from Figure 1B, the absorbance at 340 nm is in good agreement with the activity of IDO, indicating that this HILDH-coupled assay method is applicable for the screening of a large library of IDOs. As compared with previous screening methods, the method developed in this study is simple, easy-handling, time-saving, and also suitable for large-capacity random mutation library screening.

Directed Evolution of IDO to Improve the Activity toward L-Ile. Because there is no crystal structure available for the currently reported IDOs and their homologous proteins, a structure-guided rational or semirational design

https://dx.doi.org/10.1021/acs.jafc.0c06544
J. Agric. Food Chem. XXXX, XXX, XXX−XXX

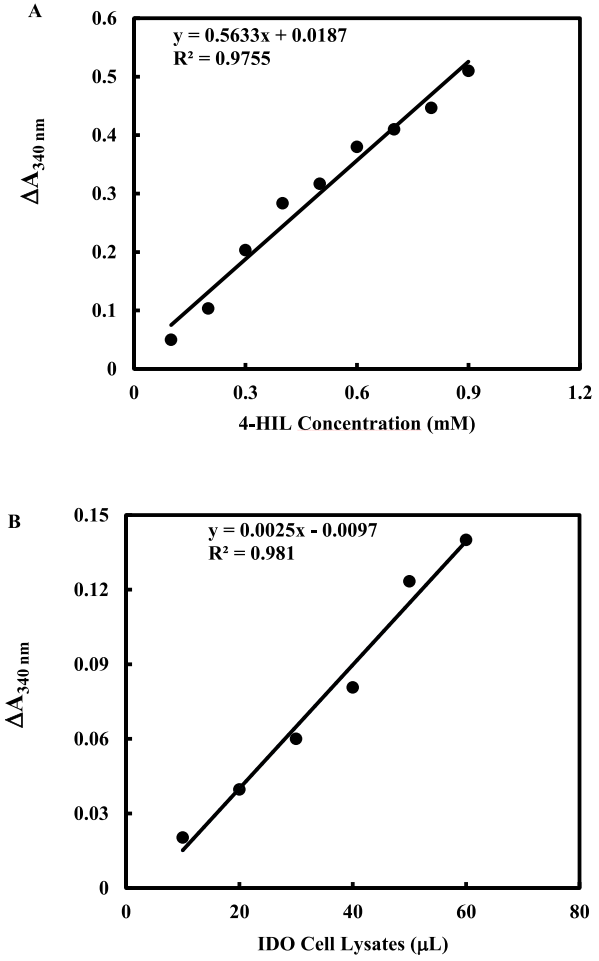

Figure 1. Validation of high-throughput screening methods. (A) Linear relationship between the concentration of 4-HIL and the absorbance at 340 nm; (B) Linear relationship between the activity of IDO and the absorbance at 340 nm.

strategy is not applicable for the engineering of IDO. Error-prone PCR-based random mutagenesis was therefore adopted for the construction of a mutant library of IDO. By screening about 20,000 clones with the high-throughput screening method developed in this study, roughly 200 clones with obvious higher catalytic activity than the wild-type IDO were chosen for rescreening in triplicate. From 200 clones, 50 clones were selected for cultivation in a shake flask and their activities toward L-Ile were measured. To this end, nine clones with activities increased from 1.5- to 3.3-fold compared to the wild-type IDO were identified and sequenced (Figure 2). The best two mutants Q38H/N155S/T182P and I162N showing a 2.8-fold and 3.3-fold enhancement in activity (cell-free extract), respectively, were subjected to nickel column affinity chromatography for further specific activity measurements (Table S5). The specific activity of I162N reached 7.3 U/mg, which is 1.9-fold higher than that of wild-type IDO, while the specific activity of Q38H/N155S/T182P was 1.3-fold higher over that of the wild-type IDO, giving 4.9 U/mg. Moreover, the protein expression levels of I162N and Q38H/N155S/T182P were both significantly improved as compared with that of the wild-type enzyme, as confirmed by SDS-PAGE analysis (Figure S1).

To figure out how the three single-point mutations contribute to the improved specific activity and protein

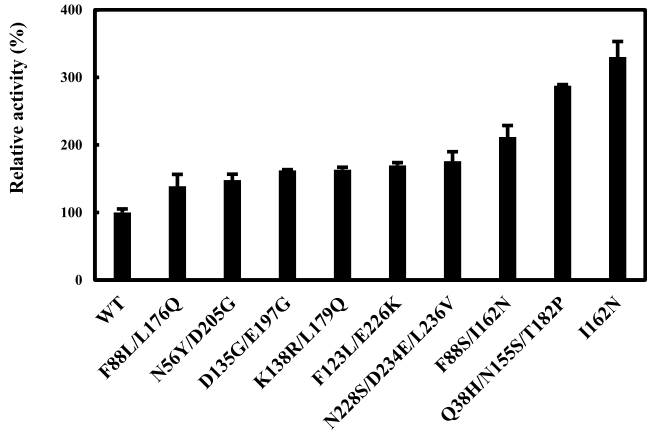

Figure 2. Comparison of the activity of the wild-type IDO and its variants.

expression level of the triple mutant Q38H/N155S/T182P, the three single-point mutants (Q38H, N155S, and T182P) were constructed, and their specific activities and protein expression levels were investigated. The improvements in specific activity of the three single-point mutants were quite similar, giving 1.2-, 1.2-, and 1.4-fold enhancement, respectively (Table S5). Gratifyingly, T182P also significantly increased the protein expression level of IDO, while the other two single-point variants did not show a prominent effect on the protein expression level (Figure S2), indicating that T182P is a key residue in determining both the specific activity and the protein expression level of IDO.

Site-Directed Saturation Mutagenesis and a Combination of Beneficial Mutations. Because residues I162 and T182 have been proven to be key determinants affecting both the specific activity and protein expression level of IDO, site-directed saturation mutagenesis was then performed at residues I162 and T182 to further investigate the influence of the other 18 amino acids on the catalytic performance of IDO. At this stage, the catalytic performance of all the variants as well as the wild-type IDO was evaluated for the biotransformation of L-Ile (228 mM) to (2*S*,3*R*,4*S*)-4-HIL on a 50 mL scale at 30 °C and pH 7.0 for 24 h using 10 g/L wet cells. For residue I162, 8 variants (D, G, A, M, L, Q, E, and P) showed lower conversion than the wild type, while the other 11 variants (T, Y, K, W, F, S, R, V, N, H, and C) exhibited higher conversion with I162T as the best mutant, giving a 47% conversion (Figure S3). In the case of T182, 6 variants (W, R, Y, D, H, and E) displayed lower conversion than the wild-type IDO, while the other 13 variants (N, G, C, F, P, L, S, M, V, A, Q, I, and K) outperformed the wild type with T182N as the best mutant, achieving up to a 70% conversion (Figure S4). The best two mutants I162T and T182N were purified to homogeneity by nickel column affinity chromatography, and their specific activities were measured, giving 6.4 and 2.8 U/mg, respectively (Table 1). Although the specific activities of I162T and T182N were lower than those of I162N (7.3 U/mg) and T182P (5.5 U/mg), respectively, higher conversions were observed with I162T and T182N in the biotransformation of L-Ile to (2*S*,3*R*,4*S*)-4-HIL (Figures S3 and S4), implying that protein expression level might play an essential role in determining their catalytic potential for the synthesis of (2*S*,3*R*,4*S*)-4-HIL. SDS-PAGE analysis revealed that the protein expression levels of I162T and T182N were substantially higher than that of the wild-type IDO (Figure 3),

https://dx.doi.org/10.1021/acs.jafc.0c06544
J. Agric. Food Chem. XXXX, XXX, XXX−XXX

Table 1. Comparison of the Activities and Expression Levels of Wild-Type IDO and its Mutants

enzyme	specific activity ($U/mg_{protein}$)	total enzyme ($mg_{Protein}/g_{Cell}$)	productivity (U/g_{Cell})
WT	3.8 ± 0.1	7.4 ± 0.4	28 ± 2
I162T	6.4 ± 0.1	21 ± 1	135 ± 2
T182N	2.8 ± 0.3	20 ± 0.2	57 ± 1
I162T/T182N	12 ± 1	21 ± 0.3	263 ± 4

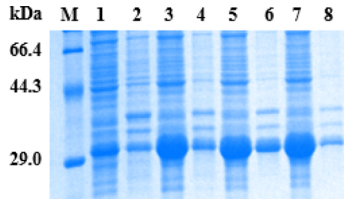

Figure 3. SDS-PAGE analysis of wild-type IDO and its mutants. Lane M: protein marker; Lane 1: supernatant of WT; Lane 2: precipitate of WT; Lane 3: supernatant of I162T; Lane 4: precipitate of I162T; Lane 5: supernatant of T182N; Lane 6: precipitate of T182N; Lane 7: supernatant of I162T/T182N; Lane 8: precipitate of I162T/T182N.

and the enzyme-specific productions of I162T and T182N reached 135 and 57 U/g_{Cells}, respectively, which were 4.8- and 2.0-fold higher than that of the wild type (28 U/g_{Cells}), respectively (Table 1). Based on these results, I162T and T182N were considered to be the best two mutants at these two positions with respect to both specific activity and protein expression level.

To investigate how the combination of these two best mutants would affect the enzyme-specific activity and protein expression level and whether there would be a synergic effect or not, a double-point mutation (I162T/T182N) was generated and its specific activity toward L-Ile and protein expression level were analyzed. The specific activity of I162T/T182N reached as high as 12 U/mg, which is 1.9-, 4.3-, and 3.2-fold higher than those of I162T, T182N, and the wild type, respectively (Table 1). In addition, the protein expression level of I162T/T182N was also significantly better than that of the wild type and comparable to those of I162T and T182N (Figure 3). Overall, the enzyme production of I162T/T182N was 9.4-fold higher than that of the wild type (Table 1). Moreover, because T182N is significantly superior to the other single variants at position Thr182, it was combined with the best four single variants at position Ile162, and the reaction progresses of the resultant four double mutants were determined, giving I162T/T182N as the best double mutant once again (Figure S5).

Enzymatic Properties of the Wild-Type IDO and Its Variant I162T/T182N. The optimal temperatures of the purified IDOs were determined at temperatures ranging from 20 to 50 °C (Figure S6). Both the wild-type IDO and its variant I162T/T182N exhibited an optimum temperature of 30 °C, and at higher temperatures (e.g., 40−50 °C), I162T/T182N displayed slightly higher activity than the wild type. The effect of pH on the activity of IDOs was also studied at pH values ranging from 5.0 to 10.0 (Figure S7). The optimum pH of 7.0 was observed for both the wild-type IDO and

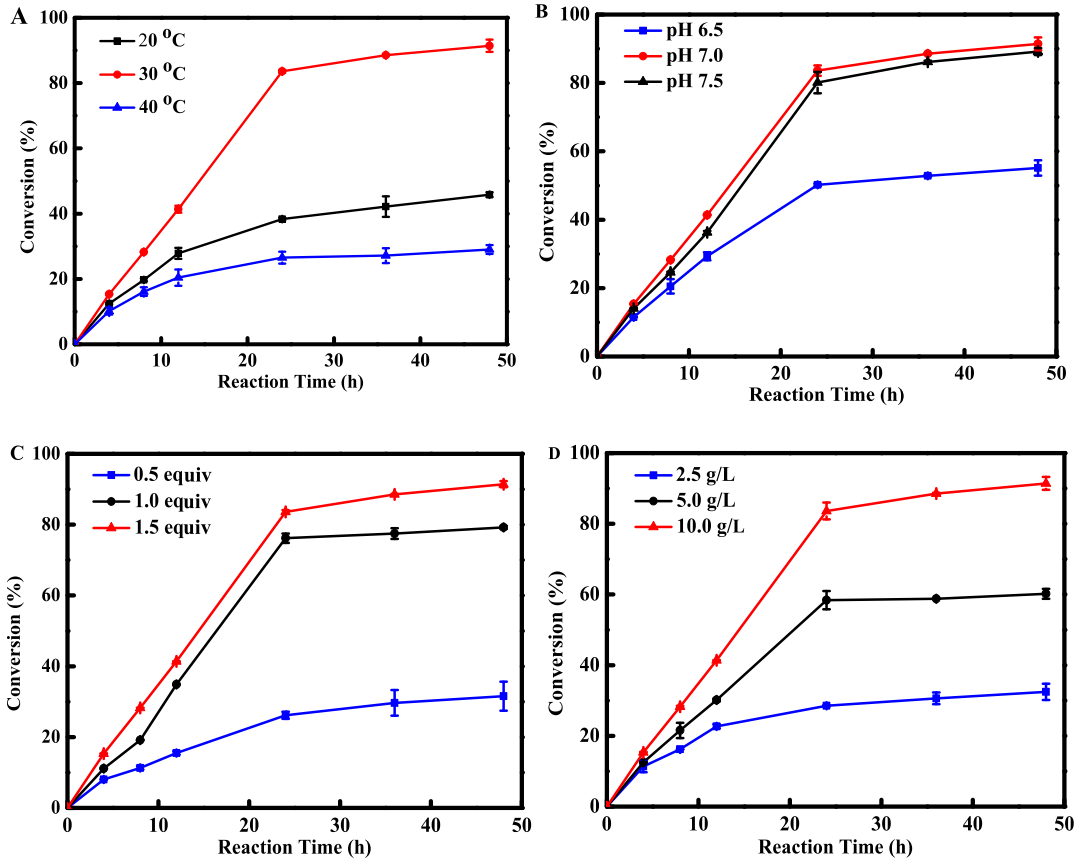

Figure 4. Optimization of reaction conditions for IDO-mediated isoleucine hydroxylation. (A) Optimization of reaction temperature; (B) optimization of reaction pH; (C) optimization of cosubstrate (α-KG) loading; (D) optimization of wet cell dosage.

https://dx.doi.org/10.1021/acs.jafc.0c06544
J. Agric. Food Chem. XXXX, XXX, XXX−XXX

I162T/T182N, and it is noteworthy that wild-type IDO showed obviously higher activity under alkaline pH conditions as compared with I162T/T182N. Meanwhile, the thermostability of IDOs was examined from 30 to 50 °C under the optimum pH (Figure S8). According to the thermal inactivation curves, the wild-type IDO displayed half-lives ($t_{1/2}$) of 35 and 11 h at 30 and 40 °C, respectively, while the variant I162T/T182N showed similar but slightly poorer thermostability than the wild type, with $t_{1/2}$ values of 25 and 3 h at 30 and 40 °C, respectively. Both IDOs dramatically lost their activities at 50 °C.

Furthermore, the influence of various metal ions and EDTA (1 mM) on the activity of IDOs was evaluated under the standard assay conditions (Table S6). The activity of IDO could be stimulated by Ca^{2+}, Mg^{2+}, and Li^{+}, whereas Mn^{2+}, Zn^{2+}, Cu^{2+}, Ni^{2+}, and Co^{2+} all completely inhibited the activity of IDO. Additionally, the activities of IDOs were entirely denatured in the presence of EDTA. These results are similar to those observed for IDO from *B. thuringiensis* 2e2 × 10^2, in which the IDO activity was completely inactivated by $ZnCl_2$, $CuCl_2$, and EDTA.[16]

Optimal Reaction Conditions for IDO-Mediated Hydroxylation of L-Ile. To improve the overall catalytic efficiency of the bioprocess, the reaction conditions for IDO-catalyzed hydroxylation of L-Ile were then optimized on a 50 mL scale with a fixed substrate concentration of 228 mM. The optimal reaction temperature of the bioprocess was determined to be 30 °C, achieving a 90% conversion after 48 h, whereas increasing or decreasing the reaction temperature significantly reduced the conversion (Figure 4A). Under the optimal reaction temperature, the IDO delivered the highest conversion of 92% at pH 7.0, and a slightly lower conversion was obtained at pH 7.5. However, at pH 6.5, only a 55% conversion was achieved (Figure 4B). Overall, the optimal reaction pH and temperature are quite similar to those of the other IDOs currently reported.[16,28−30] It should be noted that α-KG is a cosubstrate for IDO and was stoichiometrically decarboxylated to succinate during the hydroxylation of L-Ile. It can also serve as an important metabolic intermediate in the *E. coli* metabolism. Therefore, a part of α-KG added to the reaction with resting cells as biocatalysts might be utilized for the cell metabolism, thereby resulting in a low product yield.[16] The amount of α-KG was then optimized, and the highest conversion was observed with an α-KG concentration of 1.5 equiv of the substrate (Figure 4C). An approximately 80% conversion was reached using 228 mM α-KG (1.0 equiv of the substrate), and only a 30% conversion could be obtained with an α-KG concentration of 0.5 equiv of the substrate. The IDO-mediated hydroxylation of L-Ile was also carried out with different biocatalyst loadings. As can be seen from Figure 4D, the conversion depended significantly on the biocatalyst loading, and almost full conversion of L-Ile could be accomplished with 10 g/L wet cells. Reduction of biocatalyst loading dramatically decreased the conversion.

The catalytic performance of wild-type IDO and its variant I162T/T182N was then compared on a 50 mL scale under the optimal reaction conditions. As is shown in Figure 5, with the same amount of wet cells (10 g/L), 228 mM L-Ile could be completely transformed into (2*S*,3*R*,4*S*)-4-HIL after 48 h reaction by I162T/T182N, whereas the wild-type IDO gave merely a 26% conversion, highlighting the obvious better catalytic potential of the variant I162T/T182N for practical synthesis of (2*S*,3*R*,4*S*)-4-HIL.

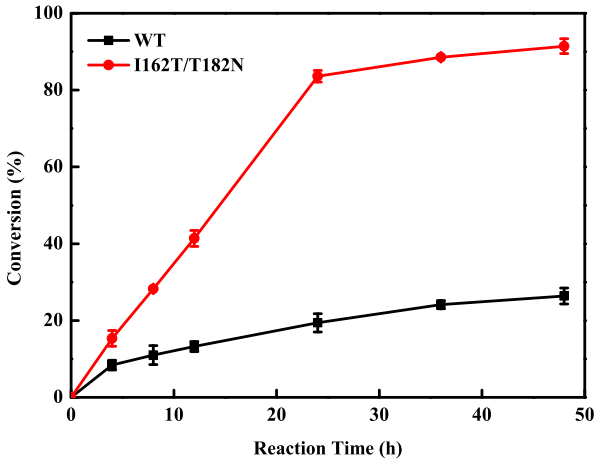

Figure 5. Reaction progress curves of L-Ile hydroxylation catalyzed by wild-type IDO and the best mutant I162T/T182N.

To further explore the catalytic potential of the variant I162T/T182N for 4-HIL biosynthesis, reactions were performed with different substrate concentrations of 228, 500, 750, and 1000 mM, respectively (Table 2). Full conversion of 228 mM L-Ile was accomplished within 10 h using 50 g/L wet cells, affording an STY as high as 80.8 g L^{-1} d^{-1}, which is approximately 2.5-fold higher than the highest value (32.1 g L^{-1} d^{-1}) reported in the literature.[30] With a further increase of the substrate concentration up to 1.0 M (131 g/L), a good conversion (>90%) could still be achieved by increasing biocatalyst loading and extending the reaction time. Additionally, the STY in all cases was still higher than the highest value reported so far. The reason for the lower conversion rate at a higher substrate concentration might be due to enzyme inactivation because a longer reaction time was required. Although great efforts have been made on the engineering of IDOs from different microorganisms for improving their catalytic efficiencies for the synthesis of (2*S*,3*R*,4*S*)-4-HIL, the enhancement was somehow limited (Table 3). For example, the double mutant (N126H/T130K) of IDO from *B. weihenstephanensis* could produce only 66.5 mM (2*S*,3*R*,4*S*)-4-HIL from 100 mM L-Ile for 24 h.[29] By using the recombinant *E. coli* cells expressing a quadruple mutant (L27I/E80D/G169H/S18D) of IDO from *B. thuringiensis* TCCC 11826 as a biocatalyst, 151.9 mM of (2*S*,3*R*,4*S*)-4-HIL was obtained from 160 mM L-Ile.[28] The best IDO for the synthesis of (2*S*,3*R*,4*S*)-4-HIL reported so far was a single-point mutation T182C from *B. subtilis* generated by introducing a disulfide bond into the protein structure, which could catalyze the formation of 191 mM (2*S*,3*R*,4*S*)-4-

Table 2. Comparison of the Reaction Results with Different Substrate Loadings[a]

substrate (mM)	catalyst (g/L)	time (h)	conversion (%)	STY (g/L/d)
228	50	10	100	80.8
500	50	48	94	34.5
750	80	48	90	49.6
1000	120	96	91	33.4

[a]Reaction conditions: the reaction mixture composed of L-Ile (228/500/750/1000 mM), $IDO_{I162T/T182N}$ (50/50/80/120 g/L, wet cells), α-KG (342/750/1250/1500 mM), Vc (10 mM), Fe^{2+} (10 mM), and 100 mM KPB (pH 7.0) was incubated at 30 °C and 200 rpm.

https://dx.doi.org/10.1021/acs.jafc.0c06544
J. Agric. Food Chem. XXXX, XXX, XXX−XXX

Table 3. Comparison of (2*S*,3*R*,4*S*)-4-HIL Synthesis with Different IDOs

biocatalyst	scale (L)	substrate (mM)	catalyst (g/L)	time (h)	conversion (%)	ref
N126H/T130K	0.1	100	200	24	67	29
L27I/E80D/G169H/S18D	0.2	160	100	12	99	28
T181C	0.2	200	50	21	95	30
$IDO_{I162T/T182N}$	0.05	228	50	10	>99	this work
$IDO_{I162T/T182N}$	3	228	10	72	94	this work

HIL from 200 mM L-Ile after 21 h reaction.[30] Therefore, we can conclude that the double mutant I162T/T182N presented in this study might serve as a promising biocatalyst for the practical production of (2*S*,3*R*,4*S*)-4-HIL in the future.

Preparative Scale Synthesis of (2*S*,3*R*,4*S*)-4-HIL. Having succeeded in improving the catalytic efficiency of IDO, preparative scale enzymatic synthesis of (2*S*,3*R*,4*S*)-4-HIL was carried out in a 5 L fermenter using the variant I162T/T182N as a biocatalyst. The pH of the reaction mixture (3 L) containing 228 mM substrate, 342 mM α-KG, 10 mM Vc, and 10 mM $FeSO_4$ was adjusted to 7.0 by 10 N NaOH before the addition of 10 g/L wet cells to initiate the reaction. The reaction temperature, agitation rate, and aeration rate were maintained at 30 °C, 200 rpm, and 1 vvm, respectively. Because of the low biocatalyst loading (10 g/L), an extended reaction time (72 h) was required to achieve a high conversion (94%), and further prolonging the reaction time did not result in a higher conversion. Because aeration was adopted to guarantee sufficient oxygen supply, this phenomenon was most likely due to inactivation of the enzyme (Figure 6 and Table 3). The total turnover number (TTN) of the biocatalyst was calculated to be as high as 30,462. The product (2*S*,3*R*,4*S*)-4-HIL was isolated by a cation-exchange resin,[34] affording 82 g of (2*S*,3*R*,4*S*)-4-HIL with a 84.2% yield (Figure S9), which corresponds to the amount of (2*S*,3*R*,4*S*)-4-HIL isolated from fenugreek seeds cultivated in an area of 252 m^2 for 9 months, further demonstrating the great potential of this IDO variant for the practical production of (2*S*,3*R*,4*S*)-4-HIL. Furthermore, the environmental factor (*E*-factor, kg waster per kg product)[35] of the bioprocess was determined to be only 2.28 with the process water excluded, highlighting the green feature of the enzymatic synthesis of (2*S*,3*R*,4*S*)-4-HIL with the IDO I162T/T182N as a biocatalyst.

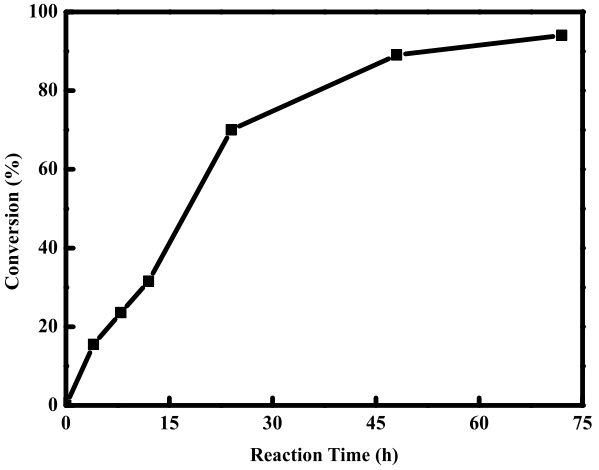

Figure 6. Reaction progress curve of the 3 L scale reaction.

The optical rotation of (2*S*,3*R*,4*S*)-4-HIL was determined, giving $[\alpha]_D^{25}$: +30.8° (*c*: 1.0 g/100 mL, solvent: H_2O), which is consistent with the data reported in the literature.[36] The structure of (2*S*,3*R*,4*S*)-4-HIL was also confirmed by ^{1}H NMR. ^{1}H NMR (600 MHz, deuterium oxide): δ/ppm 3.89 (d, J = 4.4 Hz, 1H), 3.87−3.80 (m, 1H), 1.96−1.86 (m, 1H), 1.23 (d, J = 6.3 Hz, 3H), 0.95 (d, J = 7.1 Hz, 3H) (Figure S10).

In conclusion, a high-throughput screening method was developed for the engineering of IDO from *B. subtilis*, in which a double mutant I162T/T182N was successfully identified with significantly improved specific activity and protein expression level. Under the optimal reaction conditions, by using I162T/T182N as a biocatalyst, 228 mM substrate could be completely transformed into (2*S*,3*R*,4*S*)-4-HIL with an STY of up to 80.8 g L^{-1} d^{-1}, which is the highest value reported so far. More importantly, the variant could tolerate against a substrate concentration as high as 1 M (131 g/L), and a high conversion (91%) could be achieved. Enzymatic preparation of (2*S*,3*R*,4*S*)-4-HIL was successfully carried out on a 3 L scale with a TTN of 30,462, implying great potential of this IDO variant for practical production of (2*S*,3*R*,4*S*)-4-HIL.

■ ASSOCIATED CONTENT

Supporting Information

The Supporting Information is available free of charge at https://pubs.acs.org/doi/10.1021/acs.jafc.0c06544.

PCR reaction conditions, primers used for the construction of mutant libraries, specific activity of IDO and its variants, effects of metal ions on the activity of IDO and its variants, SDS-PAGE analysis of IDO and its mutants, screening of the site-directed saturation mutagenesis libraries at positions Ile162 and Thr182, reaction progresses of the wild-type IDO and the four double mutants, effect of temperature on the activity of IDO and the mutant I162T/T182N, influence of pH on the activity of IDO and the mutant I162T/T182N, thermostabilities of IDO and the mutant I162T/T182N, and HPLC chromatogram and ^{1}H NMR of the product (2*S*,3*R*,4*S*)-4-HIL (PDF)

■ AUTHOR INFORMATION

Corresponding Authors

Zhi-Jun Zhang − *State Key Laboratory of Bioreactor Engineering, Shanghai Collaborative Innovation Centre for Biomanufacturing, School of Biotechnology, East China University of Science and Technology, Shanghai 200237, China;* orcid.org/0000-0001-9836-0204; Phone: +86-21-64252498; Email: zjzhang@ecust.edu.cn; Fax: +86-21-64250840

Hui-Lei Yu − *State Key Laboratory of Bioreactor Engineering, Shanghai Collaborative Innovation Centre for Biomanufacturing, School of Biotechnology, East China*

https://dx.doi.org/10.1021/acs.jafc.0c06544
J. Agric. Food Chem. XXXX, XXX, XXX−XXX

University of Science and Technology, Shanghai 200237, China; Email: huileiyu@ecust.edu.cn

Jian-He Xu − *State Key Laboratory of Bioreactor Engineering, Shanghai Collaborative Innovation Centre for Biomanufacturing, School of Biotechnology, East China University of Science and Technology, Shanghai 200237, China*; orcid.org/0000-0003-0140-3808; Email: jianhexu@ecust.edu.cn

Authors

Ping Du − *State Key Laboratory of Bioreactor Engineering, Shanghai Collaborative Innovation Centre for Biomanufacturing, School of Biotechnology, East China University of Science and Technology, Shanghai 200237, China*

Shuai Yan − *Department of Endocrinology and Metabolism, Shanghai General Hospital Shanghai Jiao Tong University, Shanghai 200080, China*

Xiao-Long Qian − *State Key Laboratory of Bioreactor Engineering, Shanghai Collaborative Innovation Centre for Biomanufacturing, School of Biotechnology, East China University of Science and Technology, Shanghai 200237, China*

Jiang Pan − *State Key Laboratory of Bioreactor Engineering, Shanghai Collaborative Innovation Centre for Biomanufacturing, School of Biotechnology, East China University of Science and Technology, Shanghai 200237, China*

Complete contact information is available at: https://pubs.acs.org/10.1021/acs.jafc.0c06544

Funding

This work was financially supported by the National Key Research and Development Program of China (2019YFA0905000), the National Natural Science Foundation of China (32071475, 21922804, 21672063, and 21536004), the Natural Science Foundation of Shanghai (no. 18ZR1408400), and the Fundamental Research Funds for the Central Universities (22221818014).

Notes

The authors declare no competing financial interest.

REFERENCES

(1) Fowden, L.; Pratt, H. M.; Smith, A. 4-Hydroxyisoleucine from seed of trigonella foenum-graecum. *Phytochemistry* **1973**, *12*, 1707−1711.

(2) Sauvaire, Y.; Petit, P.; Broca, C.; Manteghetti, M.; Baissac, Y.; Fernandez-Alvarez, J.; Gross, R.; Roye, M.; Leconte, A.; Gomis, R.; Ribes, G. 4-Hydroxyisoleucine: a novel amino acid potentiator of insulin secretion. *Diabetes* **1998**, *47*, 206−210.

(3) Broca, C.; Gross, R.; Petit, P.; Sauvaire, Y.; Manteghetti, M.; Tournier, M.; Masiello, P.; Gomis, R.; Ribes, G. 4-Hydroxyisoleucine: experimental evidence of its insulinotropic and antidiabetic properties. *Am. J. Physiol.* **1999**, *277*, E617−E623.

(4) Broca, C.; Manteghetti, M.; Gross, R.; Baissac, Y.; Jacob, M.; Petit, P.; Sauvaire, Y.; Ribes, G. 4-Hydroxyisoleucine: effects of synthetic and natural analogues on insulin secretion. *Eur. J. Pharmacol.* **2000**, *390*, 339−345.

(5) Sharma, R. D.; Raghuram, T. C.; Rao, N. S. Effect of fenugreek seeds on blood glucose and serum lipids in type I diabetes. *Eur. J. Clin. Nutr.* **1990**, *44*, 301−306.

(6) Narender, T.; Puri, A.; Shweta, S.; Khaliq, T.; Saxena, R.; Bhatia, G.; Chandra, R. 4-Hydroxyisoleucine an unusual amino acid as antidyslipidemic and antihyperglycemic agent. *Bioorg. Med. Chem. Lett.* **2006**, *16*, 293−296.

(7) Broca, C.; Breil, V.; Guglielmacci, C. C.; Manteghetti, M.; Rouault, C.; Derouet, M.; Rizkalla, S.; Pau, B.; Petit, P.; Ribes, G.; Ktorza, A.; Gross, R.; Reach, G.; Taouis, M. Insulinotropic agent ID-1101 (4-hydroxyisoleucine) activates insulin signaling in rat. *Am. J. Physiol. Endocrinol. Metab.* **2004**, *287*, E463−E471.

(8) Gao, F.; Jian, M. J.; Zafar, M. I.; Du, W.; Cai, Q.; Shafqat, R. A.; Lu, F. R. 4-Hydroxyisoleucine improves insulin resistance in HepG2 cells by decreasing TNF α and regulating the expression of insulin signal transduction proteins. *Mol. Med. Rep.* **2015**, *12*, 6555−6560.

(9) Ruby, B. C.; Gaskill, S. E.; Slivka, D.; Harger, S. G. The addition of fenugreek extract (trigonella foenum-graecum) to glucose feeding increases muscle glycogen resynthesis after exercise. *Amino Acids* **2005**, *28*, 71−76.

(10) Eidi, A.; Eidi, M.; Sokhteh, M. Effect of fenugreek (Trigonella foenum-graecum L) seeds on serum parameters in normal and streptozotocin-induced diabetic rats. *Nutr. Res.* **2007**, *27*, 728−733.

(11) Wang, Q.; Ouazzani, J.; Sasaki, N. A.; Potier, P. A practical synthesis of (2S,3R,4S)-4-hydroxyisoleucine, a potent insulinotropic α-mino acid from fenugreek. *Eur. J. Org. Chem.* **2002**, 834−839.

(12) Sergent, D.; Wang, Q.; Sasaki, N. A.; Ouazzani, J. Synthesis of hydantoin analogues of (2S,3R,4S)-4-hydroxyisoleucine with insulinotropic properties. *Bioorg. Med. Chem. Lett.* **2008**, *18*, 4332−4335.

(13) Claude, C.; Charles, M.; Alain, W. Preparation of diastereoisomers of 4-hydroxyisoleucine. WO 2006117696 A2, 2006.

(14) Chen, P.; Wu, C. L.; Deng, Y. Asymmetric synthesis of (2S,3R,4S)-4-hydroxyisoleucine. *Chin. J. Pharm.* **2010**, *41*, 491−494.

(15) Aouadi, K.; Jeanneau, E.; Msaddek, M.; Praly, J.-P. 1,3-Dipolar cycloaddition of a chiral nitrone to (E)-1,4-dichloro-2-butene: a new efficient synthesis of (2S,3S,4R)-4-hydroxyisoleucine. *Tetrahedron Lett.* **2012**, *53*, 2817−2821.

(16) Kodera, T.; Smirnov, S. V.; Samsonova, N. N.; Kozlov, Y. I.; Koyama, R.; Hibi, M.; Ogawa, J.; Yokozeki, K.; Shimizu, S. A novel L-isoleucine hydroxylating enzyme, l-isoleucine dioxygenase from Bacillus thuringiensis, produces (2S,3R,4S)-4-hydroxyisoleucine. *Biochem. Biophys. Res. Commun.* **2009**, *390*, 506−510.

(17) Zhang, C.; Li, Y.; Ma, J.; Liu, Y.; He, J.; Li, Y.; Zhu, F.; Meng, J.; Zhan, J.; Li, Z.; Zhao, L.; Ma, Q.; Fan, X.; Xu, Q.; Xie, X.; Chen, N. High production of 4-hydroxyisoleucine in Corynebacterium glutamicum by multistep metabolic engineering. *Metab. Eng.* **2018**, *49*, 287−298.

(18) Shi, F.; Zhang, S.; Li, Y.; Lu, Z. Enhancement of substrate supply and ido expression to improve 4-hydroxyisoleucine production in recombinant Corynebacterium glutamicum ssp. lactofermentum. *Appl. Microbiol. Biotechnol.* **2019**, *103*, 4113−4124.

(19) Kivero, A. D.; Novikova, A. E.; Smirnov, S. V. Modification of E. coli central metabolism to optimize the biotransformation of L-isoleucine into 4-hydroxyisoleucine by enzymatic hydroxylation. *Appl. Biochem. Microbiol.* **2012**, *48*, 639−644.

(20) Hibi, M.; Kawashima, T.; Kodera, T.; Smirnov, S. V.; Sokolov, P. M.; Sugiyama, M.; Shimizu, S.; Yokozeki, K.; Ogawa, J. Characterization of Bacillus thuringiensis L-isoleucine dioxygenase for production of useful amino acids. *Appl. Environ. Microbiol.* **2011**, *77*, 6926−6930.

(21) de Salas, F.; Aza, P.; Gilabert, J. F.; Santiago, G.; Kilic, S.; Sener, M. E.; Vind, J.; Guallar, V.; Martínez, A. T.; Camarero, S. Engineering of a fungal laccase to develop a robust, versatile and highly-expressed biocatalyst for sustainable chemistry. *Green Chem.* **2019**, *21*, 5374−5385.

(22) Zheng, M.-M.; Chen, K.-C.; Wang, R.-F.; Li, H.; Li, C.-X.; Xu, J.-H. Engineering 7β-hydroxysteroid dehydrogenase for enhanced ursodeoxycholic acid production by multiobjective directed evolution. *J. Agric. Food Chem.* **2017**, *65*, 1178−1185.

(23) Kong, X.-D.; Ma, Q.; Zhou, J.; Zeng, B.-B.; Xu, J.-H. A smart library of epoxide hydrolase variants and the top hits for synthesis of (S)-β-blocker precursors. *Angew. Chem., Int. Ed.* **2014**, *53*, 6641−6644.

(24) Sun, Z.; Lonsdale, R.; Kong, X.-D.; Xu, J.-H.; Zhou, J.; Reetz, M. T. Reshaping an enzyme binding pocket for enhanced and inverted stereoselectivity: use of smallest amino acid alphabets in directed evolution. *Angew. Chem., Int. Ed.* **2015**, *54*, 12410−12415.
(25) Li, G.; Zhang, H.; Sun, Z.; Liu, X.; Reetz, M. T. Multiparameter optimization in directed evolution: engineering thermostability, enantioselectivity, and activity of an epoxide hydrolase. *ACS Catal.* **2016**, *6*, 3679−3687.
(26) Li, M.; Zhang, Z.-J.; Kong, X.-D.; Yu, H.-L.; Zhou, J.; Xu, J.-H. Engineering Streptomyces coelicolor carbonyl reductase for efficient synthesis of atorvastatin precursor. *Appl. Environ. Microbiol.* **2017**, *83*, No. e00603-17.
(27) Xu, J.; Peng, Y.; Wang, Z.; Hu, Y.; Fan, J.; Zheng, H.; Lin, X.; Wu, Q. Exploiting cofactor versatility to convert a FAD-dependent Baeyer−Villiger monooxygenase into a ketoreductase. *Angew. Chem., Int. Ed.* **2019**, *58*, 14499−14503.
(28) Zhang, C.; Ma, J.; Li, Z.; Liang, Y.; Xu, Q.; Xie, X.; Chen, N. A strategy for L-isoleucine dioxygenase screening and 4-hydroxyisoleucine production by resting cells. *Bioengineered* **2017**, *9*, 72−79.
(29) Huang, S.; Shi, F. Directed evolution and site-specific mutagenesis of L-isoleucine dioxygenase derived from Bacillus weihenstephanensis. *Biotechnol. Lett.* **2018**, *40*, 1227−1235.
(30) Qiao, Z.; Xu, M.; Shao, M.; Zhao, Y.; Long, M.; Yang, T.; Zhang, X.; Yang, S.; Nakanishi, H.; Rao, Z. Engineered disulfide bonds improve thermostability and activity of L-isoleucine hydroxylase for efficient 4-HIL production in Bacillus subtilis 168. *Eng. Life Sci.* **2020**, *20*, 7−16.
(31) Ogawa, J.; Kodera, T.; Smirnov, S. V.; Hibi, M.; Samsonova, N. N.; Koyama, R.; Yamanaka, H.; Mano, J.; Kawashima, T.; Yokozeki, K.; Shimizu, S. A novel L-isoleucine metabolism in Bacillus thuringiensis generating (2S,3R,4S)-4-hydroxyisoleucine, a potential insulinotropic and anti-obesity amino acid. *Appl. Microbiol. Biotechnol.* **2011**, *89*, 1929−1938.
(32) Sánchez-Carrón, G.; Fleming, T.; Holt-Tiffin, K. E.; Campopiano, D. J. Continuous colorimetric assay that enables high-throughput screening of N-acetylamino acid racemase. *Anal. Chem.* **2015**, *87*, 3923−3928.
(33) Wilding, M.; Walsh, E. F. A.; Dorrian, S. J.; Scott, C. Identification of novel transaminases from a 12-amiondodecanoic acid-metabolizing Pseudomonas strain. *Microb. Biotechnol.* **2015**, *8*, 665−672.
(34) Zhang, Z.-J.; Cai, R. F.; Xu, J. H. Characterization of a new nitrilase from Hoeflea phototrophica DFL-43 for a two-step one-pot synthesis of (S)-*β*-amino acids. *Appl. Microbiol. Biotechnol.* **2018**, *102*, 6047−6056.
(35) Ni, Y.; Holtmann, D.; Hollmann, F. How green is biocatalysis? To calculate is to know. *ChemCatChem* **2014**, *6*, 930−943.
(36) De Lamo Marin, S.; Catala, C.; Kumar, S. R.; Valleix, A.; Wagner, A.; Mioskowski, C. A Practical and efficient total synthesis of potent insulinotropic (2S,3R,4S)-4-hydroxyisoleucine through a chiral N-protected *γ*-keto-*α*-aminoester. *Eur. J. Org. Chem.* **2010**, *21*, 3985−3989.

https://dx.doi.org/10.1021/acs.jafc.0c06544
J. Agric. Food Chem. XXXX, XXX, XXX−XXX